FEA Study of Shear Mode Decoupling in Nonstandard Thin Plates of a Lead-Free Piezoelectric Ceramic

Pilar Ochoa-Pérez, Amador Miguel González-Crespo, Álvaro García-Lucas, Francisco Javier Jiménez-Martínez, Manuel Vázquez-Rodríguez, and Lorena Pardo

***Abstract*— The finite-element analysis (FEA) is used in this work to study the impedance curves and modes of motion at resonance of nonstandard shear plates, thickness poled, and longitudinally excited. An ecological, lead-free, piezoelectric ceramic of $(1-x)(Bi_{0.5}Na_{0.5})TiO_3$–$xBaTiO_3$ with $x = 0.06$ (BNBT6) composition is studied. The FEA modeling is based on the full matrix of the material coefficients. These are obtained from complex impedance measurements on two-thickness poled resonators. A study as a function of the variations of the dimensions of the plate was accomplished (t = thickness for poling and L and w = lateral dimensions, where w is the distance between electrodes for the electrical excitation). We aimed to a further understanding, and, thus, the ability to control, the coupling of the main shear resonance and the lateral modes. The use of uncoupled shear modes to obtain the material parameters is a key issue for their determination as complex quantities, thus considering all material losses, electromechanical, dielectric, and elastic.**

***Index Terms*— Barium, bismuth, ceramics, ferroelectrics, finite element analysis (FEA), impedance, piezoelectric materials, titanium compounds.**

I. Introduction

THREE-DIMENSIONAL (3-D) modeling carried out by finite-element analysis (FEA) has become an unavoidable tool for the design of devices using piezoelectric ceramic parts [1], [2]. The seminal articles, which aroused in parallel with the microprocessor technology, are from the decade of 1970 [3], [4]. The use of FEA is due to the computational power and speed available nowadays for the calculus and the access of some piezoelectric elements in commercial finite-element codes.

Determining accurate and precise electromechanical, dielectric, and elastic properties of poled ferro-piezoelectric ceramics in the linear range and considering all losses [5], is an integral part of the way to their successful modeling by FEA. The resonance method consists in the analysis of the experimental complex impedance curves of a resonator at an electrically excited electromechanical resonance. For this, an analytical expression of the impedance as a function of the frequency is solved. This expression includes the material parameters, the density, and the dimensions of the resonator. This is the most common and standardized way for the piezoceramic properties determination. It presents the advantages of using commonly available laboratory equipment and providing great repeatability and accuracy [6]. One of the disadvantages of standard measurement methods [7] is that they require five resonator geometries for the determination of the complete matrix of coefficients of the piezoceramic. This matrix has ten independent coefficients, due to the macroscopic 6-mm symmetry induced by poling. The independent coefficients of piezoceramics are for one of the forms of the piezoelectric constitutive equations [7]: the five elastic compliances s_{11}, s_{12}, s_{13}, s_{33}, and s_{44} [since $s_{21} = s_{12}$, $s_{22} = s_{11}$, $s_{23} = s_{13}$, $s_{31} = s_{13}$, $s_{32} = s_{13}$, $s_{55} = s_{44}$, and $s_{66} = 2(s_{11} - s_{12})$]; the three piezoelectric charge coefficients d_{15}, d_{31}, and d_{33}(since $d_{32} = d_{31}$ and $d_{24} = d_{15}$); and the two dielectric permittivity components ε_{11} and ε_{33} (since $\varepsilon_{22} = \varepsilon_{11}$). Among other inconveniences, standard methods do not consider electromechanical losses. A current approach to determine losses is to define material coefficients as complex quantities [8]. Methods for determination of complex coefficients from resonance have been developed for all resonator shapes and resonance modes of relevance for material characterization and this is an ongoing topic of research [9]. The curious reader can get information on this topic in the previous works dedicated to it [5], [6], [10]–[12].

The automatic iterative [13], [14] analysis of the impedance curves at resonance is one of those methods. It combined the implementation of the software for all resonator geometries in

Manuscript received March 19, 2020; accepted May 14, 2020. Date of publication May 20, 2020; date of current version January 26, 2021. This work was supported by the Spanish Project MAT2017-86168R. *(Corresponding author: Lorena Pardo.)*

Pilar Ochoa-Pérez, Amador Miguel González-Crespo, and Francisco Javier Jiménez-Martínez are with the Department of "Electrónica Física, Ingeniería Eléctrica y Física Aplicada," ETSIST, Universidad Politécnica de Madrid (UPM), 28031 Madrid, Spain, and also with the CEMDATIC-POEMMA R&D Group, UPM, 28031 Madrid, Spain (e-mail: pilar.ochoa@upm.es; amador.m.gonzalez@upm.es; franciscojavier.jimenez@upm.es).

Álvaro García-Lucas and Lorena Pardo are with the "Instituto de Ciencia de Materiales de Madrid (ICMM)," CSIC, 28049 Madrid, Spain (e-mail: alvarog@icmm.csic.es; lpardo@icmm.csic.es).

Manuel Vázquez-Rodríguez is with the Department of "Ingeniería Telemática y Electrónica (DTE)," ETSIST, Universidad Politécnica de Madrid (UPM), 28031 Madrid, Spain, and also with the CEMDATIC-POEMMA R&D Group, UPM, 28031 Madrid, Spain (e-mail: m.vazquez@upm.es).

Digital Object Identifier 10.1109/TUFFC.2020.2996083

the full characterization with the needed calculus. It reduced the number of the required resonator geometries to only three. The resonances required were only four, namely: the length resonance of the, length poled, rod or bar; the radial and thickness resonances of the, thickness poled, thin disk; and the shear resonance of the standard thin rectangular plate, in-plane poled, and thickness excited [15].

Later on, the advantages of using nonstandard thin plates instead of standard ones for the determination of the shear parameters were revealed [16] and will be commented in the following. The nonstandard plates, here under study, are thickness poled and length excited.

First, lower electric voltages are needed for poling this resonator, which allows the characterization of materials in which this process is difficult, as the porous ceramics [17].

The dynamical clamping of the standard shear plate at inevitably coupled resonance leads to inhomogeneous strain and underestimation of the electromechanical coefficients. This undesired effect was modeled by FEA [18] and studied by laser interferometry [19]. It is worth noticing that the analysis of the shear resonance of the standard plate, which is difficult due to this unavoidable coupling of modes, is still focus of study nowadays [20], [21]. A second advantage of the nonstandard plate is that it shows a periodical coupling–decoupling from the shear resonance with other lateral modes. This was observed as the aspect ratio (w/t = length for excitation/thickness for poling) was increased. The periodical coupling–decoupling was experimentally determined for a commercial lead titanate-zirconate (PZT) [22] and $Ba_{1-x}Ca_xTi_{0.90}Zr_{0.10}O_3$ (BCZT), where $x = 0.15$, lead-free piezoceramic [23]. This periodicity allows effective decoupling of the shear mode of the plate by controlled reduction of the thickness of the plate. The uncoupled shear mode provides the accurate, complex impedance data which are needed, in addition to the characteristic frequencies, for determining material coefficients as complex quantities, thus considering all losses.

A third advantage of the rectangular shear resonator studied here is that it could be cut out of a, thickness poled, thin disk after the parameter's determination from its radial, and thickness resonance modes. Similarly, the long bar, longitudinally poled, could be also cut out of the disk. These facts could reduce the number of resonators for complete characterization by the resonance method to only one, thin disk, thickness poled. However, the procedure includes cutting and repoling it in a long direction [24]. This is not recommended as it has to be done with extreme care in order to avoid damaging the ceramic. Instead, it was recently shown that it is possible to obtain the full matrix of coefficients using only two resonator geometries [25], namely, the disk and shear plate, thickness poled. The coefficients that should be obtained by analysis of the, longitudinally poled, rod or bar [15] were instead determined from a wide impedance spectrum of the thin disk [25]. For this, an alternative methodology was used. The complex impedance spectrum, from the radial mode, its overtones, the thickness mode and some other modes close to it, was measured and

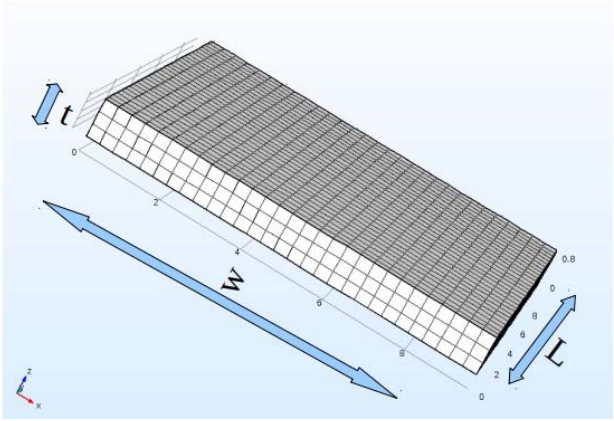

Fig. 1. FEA model of the nonstandard shear plate, thickness poled, and longitudinally excited (t = thickness for poling and w = distance between electrodes for the electrical excitation).

the modes were identified. A first model of the spectrum was made, using a specific FEA code [12] for this purpose, and based on the data from the automatic iterative analysis of the two thickness-poled resonators mentioned. After a sensitivity study of different parameters on the model, the difference between the numerical and experimental data was minimized and the full set of complex coefficients were obtained [25].

FEA is used in this work to study the impedance curves and modes of motion at resonance of, thickness poled and longitudinally excited, nonstandard plates as a function of the change of its dimensions (Fig. 1). We aim to check reproducibility, general character, and independence of artifacts of the experimentally observed coupling–decoupling phenomenon as the thickness of the plate is reduced and in the case of a material not yet studied in this regard [26]. Besides, by modeling, it was also possible to the study all the dimensional changes potentially affecting the aspect ratio of the plate. This study, otherwise costly for many samples are required, involves the changes in thickness for poling, width for excitation, and length of the plate. The final purpose of this work is to gain a further understanding and the ability to control decoupling of this resonator.

II. Experimental Methods

A. Material

A ceramic obtained from nanopowders [26] with composition $(1 - x)(Bi_{0.5}Na_{0.5})TiO_3$–$xBaTiO_3$ with $x = 0.06$ (BNBT6) was selected for this study. This is a widely studied material and its matrix characterization was readily available [25]. For the sake of this study, a ceramic plate of the initial dimensions ($w \times L \times t$) of $9.53 \times 9.43 \times 0.89$ mm^3 and density 5.49 g·cm^{-3} was made as explained elsewhere [26]. The complex impedance was measured using an impedance analyzer (model HP4192A-LF impedance analyzer, Hewlett Packard, Palo Alto, CA, USA). The plate thickness was reduced in 0.02-mm steps and the impedance measured again, so as to obtain two spectra, with ($t = 0.89$ mm) and without ($t = 0.83$ mm) coupling with lateral modes. These measurements were used to check the validity of the FEA results.

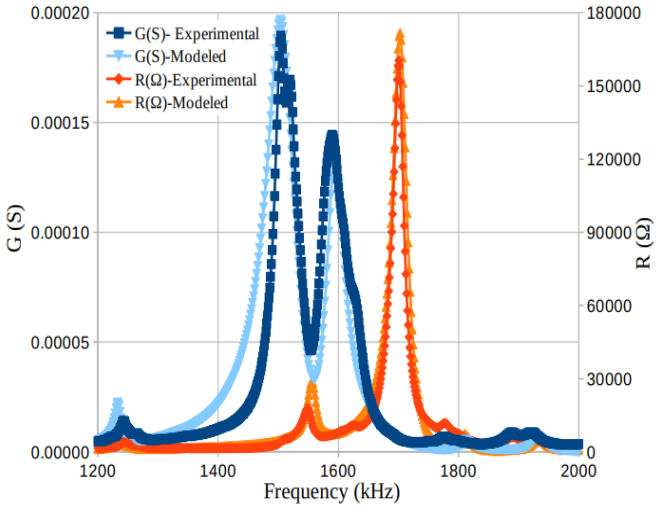

Fig. 2. Complex impedance, plotted as conductance (G) and resistance (R) peaks, of a nonstandard plate of BNBT6 of 9.53 × 9.43 × 0.89 mm^3. Experimental data as well as FEA calculated peaks are shown.

B. Finite-Element Analysis

COMSOL Multiphysics V5.2 FEA modeling software was used here. The piezoelectric device module (PZD) was used to simulate the piezoelectric response of the plates. The 3-D structural mechanics module has been used to simulate the mechanical response in the frequency domain. The mesh used was selected so as to have five nodes per wavelength, which allowed simulating modes of resonance that are excited together with the main shear resonance. The convergence criterion of the FEA analysis was the reproduction of the experimental results previously mentioned above. The number of frequencies analyzed was chosen so as to get a high resolution of each calculated spectra. The shear plate was simulated as a full 3-D item. This results in, typically, 1–5 h calculation time for each sweep of 200–1000 frequencies, respectively. The 3-D harmonic analysis, used here, yields the complex impedance values in a given interval of frequencies and the modes of motion at each frequency. The intervals of the frequency of interest in this work were those of the experimental results. The dimensional changes modeled here were: 1) w from 8.7 to 10.35 mm, $L = 9.43$ mm, and $t = 0.89$ mm; 2) L from 8.0 to 10.5 mm, $w = 9.53$ mm, and $t = 0.89$ mm; and 3) t from 0.85 to 1.10 mm, $w = 9.53$ mm, and $L = 9.43$ mm.

C. Determination of the Matrix of Complex Material Coefficients

An initial FEA calculation of the complex impedance of the shear plate showing mode coupling ($t = 0.89$ mm) was made based on the material coefficients determined in [25].

Complex impedance was plotted as the peaks of the resistance (R), real part of the impedance, and conductance (G), real part of the inverse of the impedance, the admittance. Coefficients were slightly adapted, considering the deviation of the experimental measurements, for an optimum reproduction of the shear impedance spectra of the plate. The frequencies as well as the height and width of all the G and R peaks, of the shear and lateral resonance modes were well determined (Fig. 2). This set of coefficients shown in Table I was used for all the calculations showed here.

TABLE I
TEN INDEPENDENT BNBT6 COEFFICIENTS USED IN THE FEA MODEL

Quantity (units)	Value
$s^E_{11}(10^{-12}$ m^2/N)	8.774 - 0.079i
s^E_{12} "	-2.190 + 0.021i
s^E_{13} "	-2.750 + 0.024i
s^E_{33} "	9.889 - 0.090i
s^E_{55} "	24.729 - 1.222i
d_{31} (10^{-12} C/N)	- 35.18 + 0.63i
d_{33} "	101.81 - 1.87i
d_{15} "	203.25 – 24,85i
ε^T_{11} (ε_0)	774 - 43i
ε^T_{33} "	534 - 15i

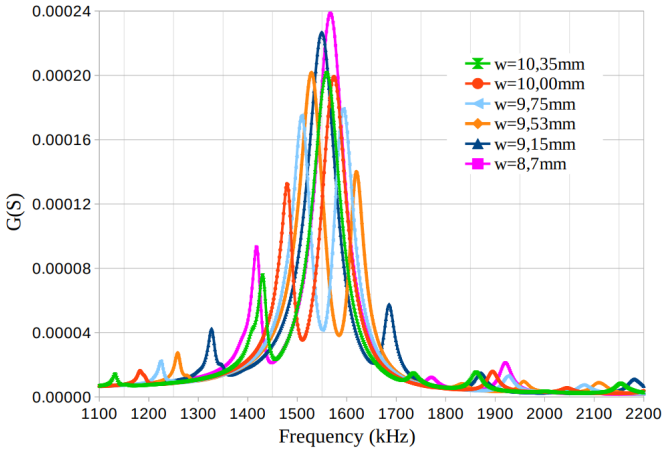

Fig. 3. FEA modeled conductance (G) peaks as the distance between electrodes was changed from 8.7 to 10.35 mm and the lateral dimension (L) and thickness (t) of a nonstandard plate of BNBT6 were keep constant.

III. RESULTS AND DISCUSSION

A. Electrical Impedance

1) Variation of the Distance Between Electrodes for the Electrical Excitation of the Electromechanical Resonance (w): Figs. 3 and 4 show the modeled peaks of G and R, respectively, for the plates as a function of the lateral dimension w.

An increase of the frequency of the peaks of the lateral mode as w decreases is observed below 1500 kHz, where the antiresonance does not affect them. This sequence is observed for two sets of peaks and it is clearer in Fig. 4. This shows that w is the main dimension of the plate that drives these lateral modes. The closer the frequency of the lateral resonance is to the main shear one, the more intense is the corresponding G and R peaks. This is due to the energy transfer between resonances when coupling takes place.

2) Variation of the Lateral Dimension of the Plate (L): Figs. 5 and 6 show the G and R peaks, respectively, of the plate under study as a function of the lateral dimension from 8.0 to 10.5 mm. It is apparent that changes of L do not affect significantly neither the frequency of the main shear resonance

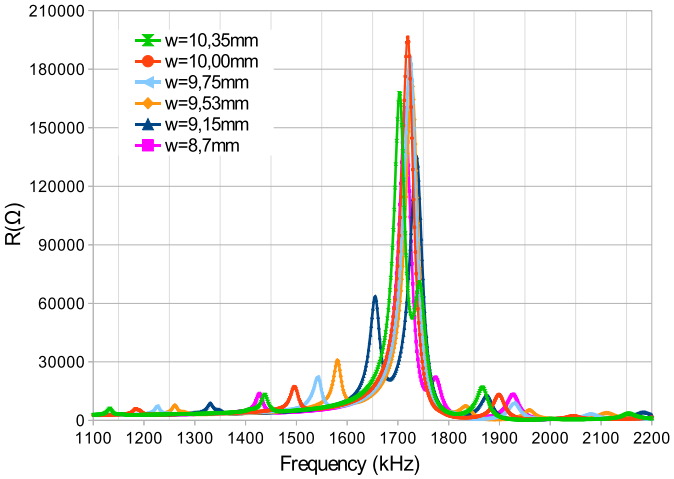

Fig. 4. FEA modeled resistance (R) peaks as the distance between electrodes was changed from 8.7 to 10.35 mm for constant t and L of a nonstandard plate of BNBT6.

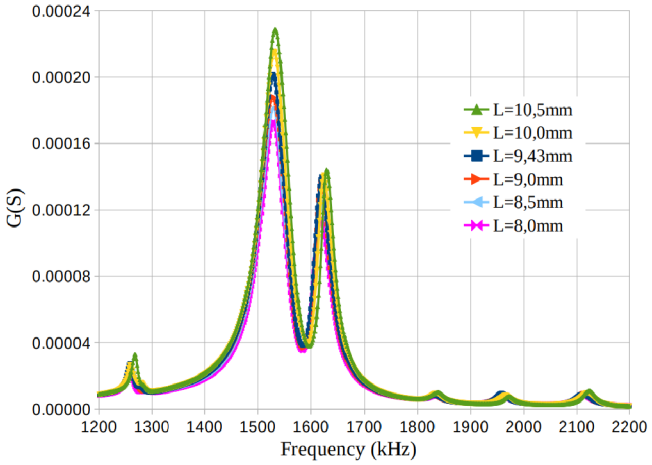

Fig. 5. FEA modeled conductance (G) peaks of a nonstandard, thickness poled, and length excited, plate of BNBT6 as the lateral dimension L was changed from 8.0 to 10.5 mm with constant $w = 9.53$ mm and $t = 0.89$ mm.

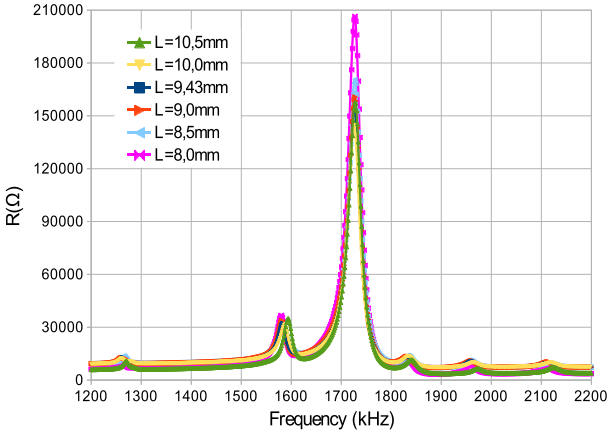

Fig. 6. FEA modeled resistance (R) peaks of a nonstandard plate of BNBT6 as the lateral dimension L was changed from 8.0 to 10.5 mm with constant $w = 9.53$ mm and $t = 0.89$ mm.

nor that of the lateral modes at both sides of it. However, for an increase of L, the electrode area ($L \times t$) increases. Consequently, the capacitance of the resonator increases, as well and its admittance, which changes the height of the G and R peaks.

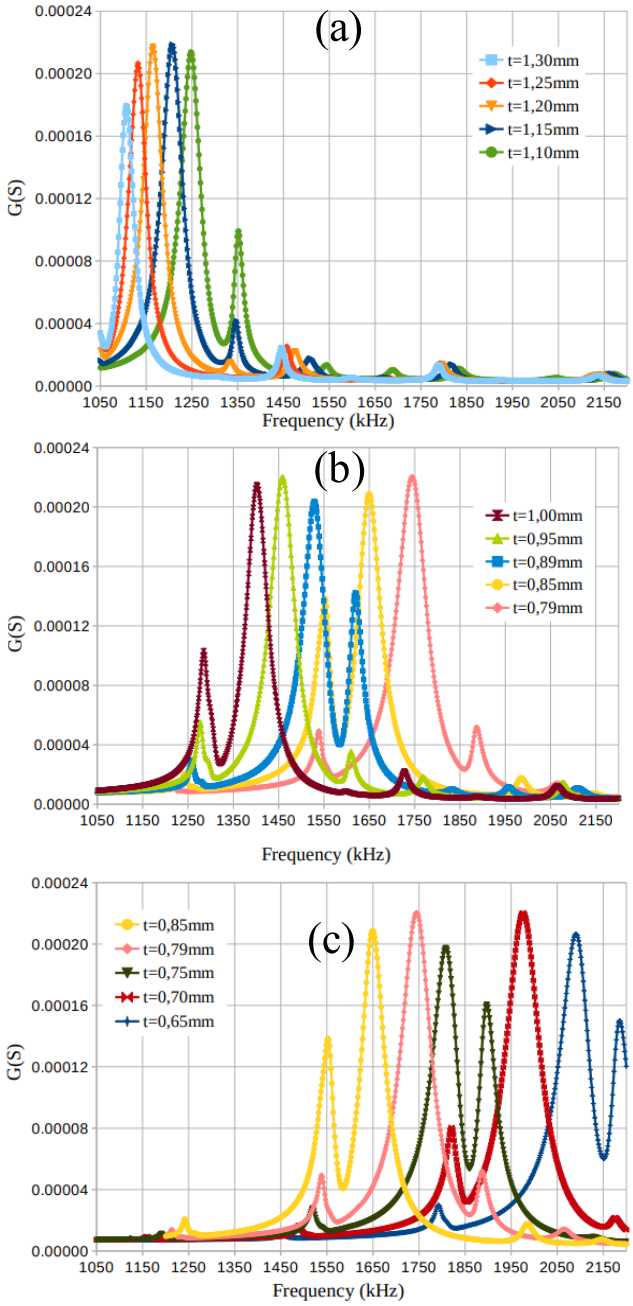

Fig. 7. FEA modeled conductance (G) peaks (resonance) of a plate of BNBT6 as the thickness changes with constant $w = 9.53$ mm and $L = 9.43$ mm. (a) $1.30 < t < 1.10$ mm. (b) $1.00 < t < 0.79$ mm.(c) from $0.85 < t < 0.65$ mm.

3) Variation of the Thickness for Poling (t): The results of the FEA in Figs. 7 and 8 reproduce well for BNBT the phenomena previously observed experimentally for PZT [22] and for a BCZT lead-free ceramic [23], showing its general character and that it is not a result of an experimental artifact. As the thickness of the plate is reduced, the main shear resonance takes place at higher frequency, meaning that this is a thickness-driven resonance. As it was already observed from Figs. 3–6, a number of lateral modes take place at almost constant intervals of frequency. These have very weak intensity when taking place away from the frequency of the main shear resonance. However, they are also mechanically excited by the

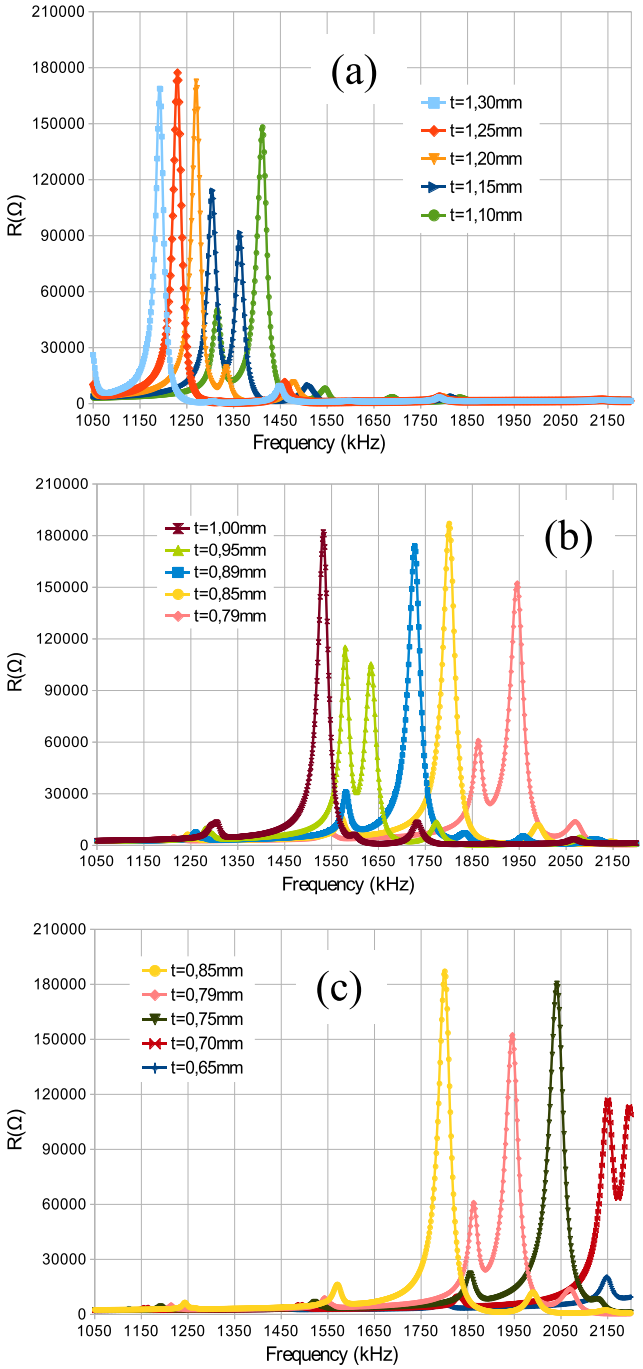

Fig. 8. FEA modeled resistance (R) peaks (resonance) of a nonstandard plate of BNBT6 as the thickness changes with constant w and L. (a) $1.30 < t < 1.10$ mm. (b) $1.00 < t < 0.79$ mm. (c) from $0.85 < t < 0.65$ mm.

shear movement when their frequency matches the frequency of the, electrically excited, shear resonance, and the coupling of resonances takes place. This also produces a slight change of frequency in the lateral modes, which can be seen, e.g., nearly 1450 kHz in Fig. 8(a).

The periodic coupling–decoupling phenomenon occurs three times in the analyzed frequency range [for $1.30 > t(\text{mm}) > 0.95$, $0.95 > t(\text{mm}) > 0.79$, and $0.79 > t(\text{mm})$ in Fig. 7]. For both extreme values of these intervals, it can be

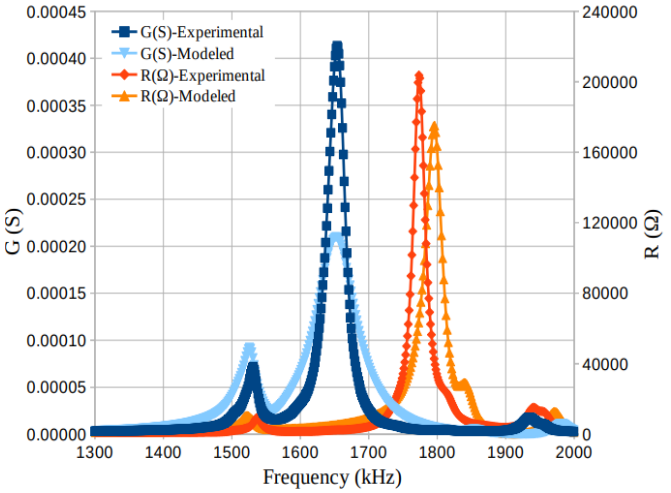

Fig. 9. Complex impedance, plotted as conductance (G) and resistance (R) peaks of a nonstandard plate of BNBT6 and $9.53 \times 9.43 \times 0.83$ mm^3 (aspect ratio 11.48). Experimental data as well as FEA calculated peaks are shown.

seen a resolved shear resonance G peak, while double peaks are observed in the middle of the interval. The R peak for $t = 1.30$ mm is also resolved, which provides the required unique resonance to analyze for the determination of the material coefficients. However, as the thickness decreases, the G and R peaks become wider and to get the proper thickness for an uncoupled shear resonance is more difficult.

For $t = 0.95$ mm [Fig. 8(b)], the double R peak shows clearly that coupling with the following lateral mode, has been reached. Therefore, in this thickness range, the uncoupled shear mode is obtained in the intervals from $1.00 > t(\text{mm}) > 0.95$ to $0.85 > t(\text{mm}) > 0.79$. Given the value of $w = 9.53$ mm, these conditions for uncoupled shear modes correspond to aspect ratios (length for excitation/thickness for poling) of $7.33, 9.53 < w/t < 10.03$, and $11.22 < w/t < 12.06$. Indeed, the prediction of the FEA results is in agreement with the experimental spectrum measured (Fig. 9) for the ceramic sample of BNBT6 with $t = 0.83$ mm ($w/t = 11.48$). The small changes of material parameters required for the optimum modeling of the coupled spectra (Fig. 2) explain the differences between the FEA calculated and the experimental spectra in Fig. 9, where, nevertheless, the uncoupled spectra is reproduced.

Due to the mechanical characteristics of piezoceramic samples, which are brittle materials, the range of achievable aspect ratios with bulk ceramic resonators is not unlimited. Those here shown from the thickness interval studied in Figs. 7 and 8 are feasible with BNBT6 ceramics. However, the EMAS6100 Standard [27] recommendation for standard shear plates, in-plane poled, is that the aspect ratio (length for poling/thickness for excitation) of the shear mode must be larger than 32. This will mean with our actual samples a thickness smaller than 0.30 mm, to suppress the spurious peaks. Besides, even for such a high aspect ratio, secondary modes are not eliminated, but their coupling with the primary, thickness-driven shear mode is reduced [28]. Therefore, the results in Figs. 7 and 8 reproduce the coupling–decoupling phenomenon that was experimentally observed. They also show that it takes place

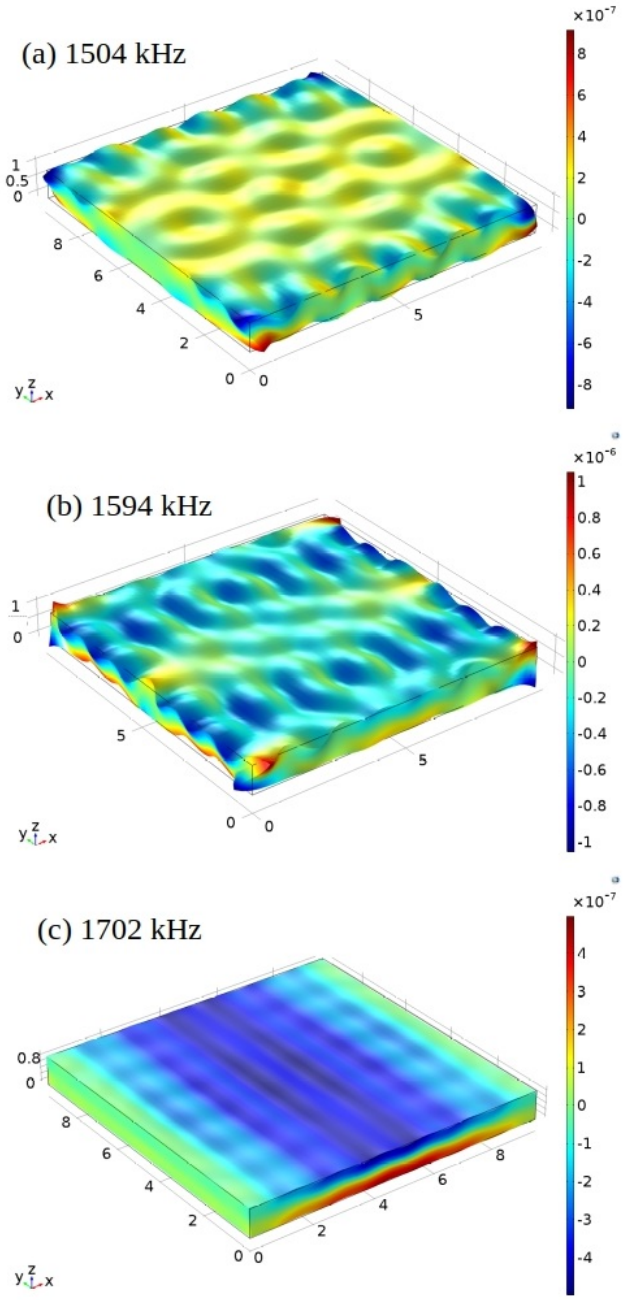

Fig. 10. 3-D representation of the motion at three characteristic frequencies of the impedance spectra of the BNBT6 plate of 0.89-mm thickness showed in Fig. 2: the frequencies for the maxima of the two G peaks, (a) 1504 kHz, (b) 1594 kHz, and (c) 1702 kHz, the frequency for the maximum R.

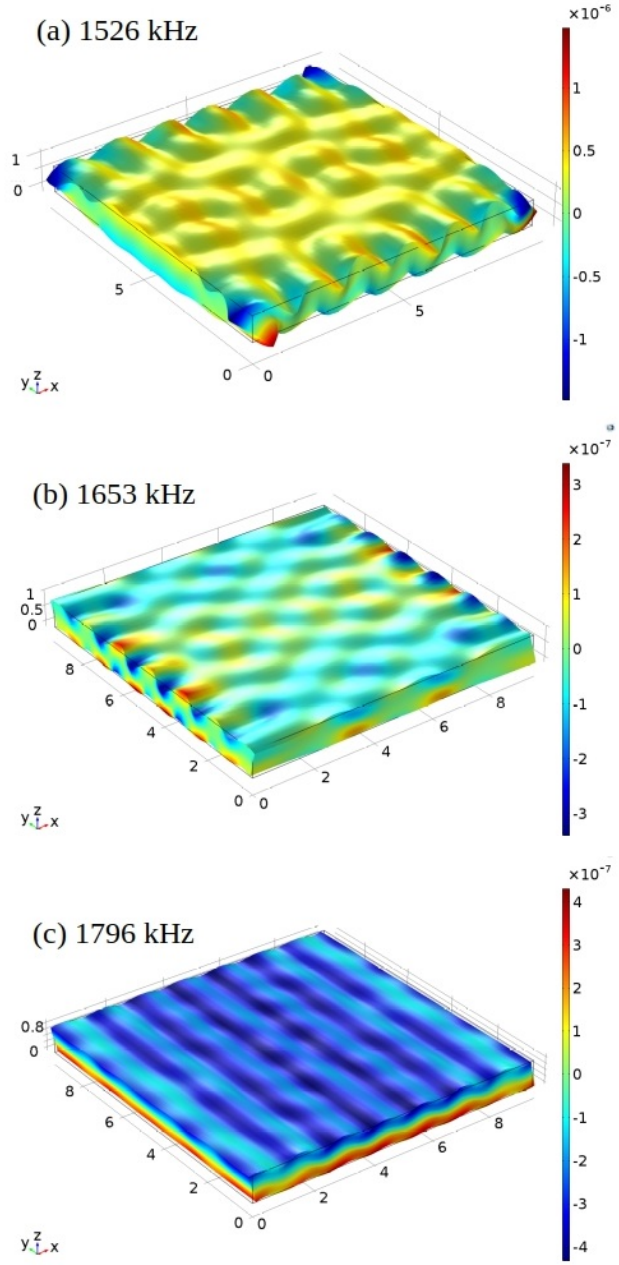

Fig. 11. 3-D plots of the motion at the characteristic frequencies of the impedance spectrum of the BNBT6 plate of 0.83-mm thickness showed in Fig. 9. (a) 1526 kHz, the frequencies for the maximum of the G peak for a lateral mode. (b) 1653 kHz, the frequencies for the maximum of the G peak for the shear mode. (c) 1796 kHz, the frequency for the maximum R.

for realizable aspect ratios of the nonstandard shear plate. This was achieved without using a large number of samples.

B. Modes of Motion

In order to get an insight on the modes of motion at resonance, Figs. 10 and 11 show the displacement field. The color scale indicates the magnitude (in millimeters) and the direction in the x-axis of the displacement in each point of the plate. The displacement in the 3-D representation is the actual one amplified by a factor of 3×10^5.

Fig. 10 shows the movements of the BNBT6 plate of dimensions ($w \times L \times t$) $9.53 \times 9.43 \times 0.89$ mm^3. The frequencies of 1504 and 1594 kHz correspond to the two maxima of the G spectrum (electrical resonances), and the frequency of 1702 kHz corresponds to the maximum at the R spectrum (electrical antiresonance), that are shown at Fig. 2, which is an example of mode coupling.

For 1504 kHz [Fig. 10(a)], an inhomogeneous mode of movement is observed with standing waves in both plate edges in the x-direction (w = distance between electrodes) and with a strong interference pattern in the plane of the plate. Also, the deformation at the four twisted corners of the plate shows shear movement with components in all three axes. At 1594 kHz, we found the still strong influence of the lateral modes on the plate movement [Fig. 10(b)].

The dominating lateral waves are at the electrode edges of the plate in Fig. 10(b), and they have overall higher displacements at the interference pattern than in Fig. 10(a). Fig. 10(b) also shows a mirror plane perpendicular to the *xy*-plane and the electrodes.

For 1702 kHz [Fig. 10(c)], at the electrical antiresonance, we obtain the expected, virtually pure, shear movement with little out-of-plane displacement in the z-direction. However, it is noticeable that near the electrodes, there are layers with low displacement and that movement increases toward the center of the plate. That is to say that the plate shows some extend of dynamic clamping and inhomogeneous motion, which should lead to underestimation of electromechanical parameters from the spectra in Fig. 2. Indeed, this was previously observed experimentally for standard plates [18], [19].

Fig. 11 shows the movements of the BNBT6 plate of dimensions ($w \times L \times t$) 9.53 × 9.43 × 0.83 mm^3. The frequencies of 1526 and 1653 kHz correspond to the two maxima of the G spectrum (electrical resonances), for the lateral and the shear mode, respectively. The frequency of 1702 kHz corresponds to the maximum at the R spectrum (electrical antiresonance) for the shear mode. These are shown in Fig. 9, where an uncoupled shear mode is observed.

Fig. 11(a) and (b) shows the same modes of motion of the plate described previously in Fig. 10(a) and (b). It reveals, due to the decoupling of modes, that the motion of the standing wave for the lateral resonance at 1526 kHz [Fig. 10(a)] occurs with a higher displacement. It also shows that the main shear resonance at 1653 kHz [Fig. 11(b)] occurs with a lower distortion caused by a lateral resonance. Finally, Fig. 11(c) reveals a shear movement that occurs homogeneously at the whole plate, without clamping, and with a minor component of out-of-plane displacement.

It must be noticed that the study of vibrations of plates is a complicated field [29] and a more detailed or analytical description of these modes of movement is itself a project, which is out of the scope of this work. However, here we are concerned with the use of nonstandard piezoceramic plates for material characterization. In this article, the comparison of results in Figs. 10 and 11 reveals the dynamical clamping [Fig. 10(c)] of the shear mode when coupling with lateral modes takes place, which leads to the experimentally observed underestimation of the shear parameters [18]. These results also confirm that a virtually free, unclamped, shear resonance [Fig. 11(c)] can be achieved by the effective reduction of the thickness of the plate.

IV. Conclusion

COMSOL Multiphysics V5.2 commercial FEA software was used for modeling of the complex impedance spectrum and modes of motion at resonance of nonstandard piezoceramic plates, thickness poled, and longitudinally excited. Modeling was accomplished as a function of the change of all plate dimensions (t = thickness for poling, L, and w = lateral dimensions, where w = distance between electrodes for the electrical excitation). The FEA was based on a full matrix of BNBT6 coefficients as complex quantities (Table I), thus considering all material losses. The determination of all these coefficients was made from measurements on only two resonators: thickness poled thin disk and plate. A plate of composition $(1-x)(Bi_{0.5}Na_{0.5})TiO_3$–$xBaTiO_3$ with $x = 0.06$ (BNBT6), not yet studied in this regard, was selected for this work. Experimental values of complex impedance at the shear resonance were used to check the validity of the FEA results.

The results of the FEA calculations show that w is the main dimension of the plate controlling the frequencies at which the secondary lateral modes take place. L does not affect significantly, neither the frequency of the main shear resonance nor that of the lateral modes at both sides of it. However, for an increase of L, the electroded area ($L \times t$) increases as well and it leads to small changes in the impedance of the resonator.

The periodic coupling–decoupling phenomenon that was observed experimentally as the thickness for poling, t, is reduced can be well reproduced by FEA for its control without the need of a large number of samples. Besides, it also takes place for realizable aspect ratios (length for excitation/thickness for poling, w/t) of the nonstandard shear plate. For the BNBT6 shear plate analyzed here, uncoupled modes are found for $w/t = 7.33$ and in the intervals of $9.53 < w/t < 10.03$ and $11.22 < w/t < 12.06$. These aspect ratios are much lower than those needed for the use of standard shear plates (length for poling/thickness for excitation > 32).

The FEA modeled modes of motion at relevant frequencies, for both the coupled and uncoupled impedance spectra, of the BNBT6 plates confirm that homogeneous shear modes of movement are obtained when an uncoupled shear resonance of the plate takes place.

References

[1] A. Benjeddou, "Advances in piezoelectric finite element modeling of adaptive structural elements: A survey," *Comput. Struct.*, vol. 76, nos. 1–3, pp. 347–363, 2000, doi: 10.1016/S0045-7949(99) 00151-0.

[2] H. A. Kunkel, S. Locke, and B. Pikeroen, "Finite-element analysis of vibrational modes in piezoelectric ceramic disks," *IEEE Trans. Ultrason., Ferroelectr., Freq. Control*, vol. 37, no. 4, pp. 316–328, Jul. 1990, doi: 10.1109/58.56492.

[3] H. Allik and T. J. R. Hughes, "Finite element method for piezoelectric vibration," *Int. J. Numer. Methods Eng.*, vol. 2, no. 2, pp. 151–157, Apr. 1970, doi: 10.1002/nme.1620020202.

[4] Y. Kagawa, "A new approach to analysis and design of electromechanical filters by finite-element technique," *J. Acoust. Soc. Amer.*, vol. 49, no. 5A, pp. 1348–1356, May 1971, doi: 10.1121/1.1912508.

[5] A. González, Á. García, C. Benavente-Peces, and L. Pardo, "Revisiting the characterization of the losses in piezoelectric materials from impedance spectroscopy at resonance," *Materials*, vol. 9, no. 2, p. 72, Jan. 2016, doi: 10.3390/ma9020072.

[6] J. Fialka and P. Benes, "Comparison of methods for the measurement of piezoelectric coefficients," *IEEE Trans. Instrum. Meas.*, vol. 62, no. 5, pp. 1047–1057, May 2013, doi: 10.1109/TIM.2012.2234576.

[7] Publication and Proposed Revision of ANSI/IEEE Standard 176-1987, "ANSI/IEEE standard on piezoelectricity," *IEEE Trans. Ultrason., Ferroelectr., Freq. Control*, vol. 43, no. 5, pp. 717–718, Sep. 1996, doi: 10.1109/TUFFC.1996.535477.

[8] R. Holland, "Representation of dielectric, elastic, and piezoelectric losses by complex coefficients," *IEEE Trans. Sonics Ultrason.*, vol. SU-14, no. 1, pp. 18–20, Jan. 1967, doi: 10.1109/T-SU.1967.29405v.

[9] A. Mezheritsky, "Q-factor spectrum of a piezoceramic resonator and method for piezoelectric loss factor determination," *IEEE Trans. Ultrason., Ferroelectr., Freq. Control*, vol. 64, no. 12, pp. 1849–1856, Dec. 2017, doi: 10.1109/TUFFC.2017.2748901.

[10] K. Wing Kwok, H. L. W. Chan, and C. L. Choy, "Evaluation of the material parameters of piezoelectric materials by various methods," *IEEE Trans. Ultrason., Ferroelectr., Freq. Control*, vol. 44, no. 4, pp. 733–742, Jul. 1997, doi: 10.1109/58.655188.

[11] L. Pardo and K. Brebøl, "Properties of ferro-piezoelectric ceramic materials in the linear range: Determination from impedance measurements at resonance," in *Multifunctional Polycrystalline Ferroelectric Materials*, L. Pardo and J. Ricote, Eds. Cham, Switzerland: Springer, 2011, pp. 617–649.

[12] N. Pérez, F. Buiochi, M. Brizzotti Andrade, and J. Adamowski, "Numerical characterization of piezoceramics using resonance curves," *Materials*, vol. 9, no. 2, p. 71, Jan. 2016, doi: 10.3390/ma9020071.

[13] C. Alemany, L. Pardo, B. Jiménez, F. Carmona, J. Mendiola, and A. M. González, "Automatic iterative evaluation of complex material constants in piezoelectric ceramics," *J. Phys. D, Appl. Phys.*, vol. 27, no. 1, pp. 148–155, 1994, doi: 10.1088/0022-3727/27/1/023.

[14] C. Alemany, A. M. Gonzalez, L. Pardo, B. Jimenez, F. Carmona, and J. Mendiola, "Automatic determination of complex constants of piezoelectric lossy materials in the radial mode," *J. Phys. D, Appl. Phys.*, vol. 28, no. 5, pp. 945–956, May 1995, doi: 10.1088/0022-3727/28/5/017.

[15] M. Algueró, C. Alemany, L. Pardo, and A. M. González, "Method for obtaining the full set of linear electric, mechanical, and electromechanical coefficients and all related losses of a piezoelectric ceramic," *J. Amer. Ceram. Soc.*, vol. 87, no. 2, pp. 209–215, Feb. 2004, doi: 10.1111/j.1551-2916.2004.00209.x.

[16] L. Pardo, M. Algueró, and K. Brebøl, "A non-standard shear resonator for the matrix characterization of piezoceramics and its validation study by finite element analysis," *J. Phys. D, Appl. Phys.*, vol. 40, no. 7, pp. 2162–2169, Apr. 2007, doi: 10.1088/0022-3727/40/7/046.

[17] L. Pardo, A. García, K. Brebøl, D. Piazza, and C. Galassi, "Key issues in the characterization of porous PZT based ceramics with morphotropic phase boundary composition," *J. Electroceram.*, vol. 19, no. 4, pp. 413–418, Dec. 2007, doi: 10.1007/s10832-007-9050-5.

[18] L. Pardo, M. Algueró, and K. Brebøl, "Resonance modes in the standard characterization of ferro-piezoceramic samples: A discussion based on modelling by finite element analysis," *Ferroelectrics*, vol. 336, no. 1, pp. 181–190, Jul. 2006, doi: 10.1080/00150190600739996.

[19] L. Pardo, F. Montero de Espinosa, and K. Brebøl, "Study by laser interferometry of the resonance modes of the shear plate used in the standards characterization of piezoceramics," *J. Electroceram.*, vol. 19, no. 4, pp. 437–442, Dec. 2007, doi: 10.1007/s10832-007-9052-3.

[20] M. Brissaud, "Modelling and characterisation of shear modes of rectangular piezoelectric materials," *Ferroelectrics*, vol. 550, no. 1, pp. 12–35, Oct. 2019, doi: 10.1080/00150193.2019.1652494.

[21] M. Brissaud, "Modelling of coupling between shear and longitudinal modes of a bulky rectangular piezoelectric element," *Mater. Res. Exp.*, vol. 6, no. 9, Jun. 2019, Art. no. 095701, doi: 10.1088/2053-1591/ab2a5d.

[22] L. Pardo, A. García, F. M. De Espinosa, and K. Brebøl, "Shear resonance mode decoupling to determine the characteristic matrix of piezoceramics for 3-D modeling," *IEEE Trans. Ultrason., Ferroelectr., Freq. Control*, vol. 58, no. 3, pp. 646–657, Mar. 2011, doi: 10.1109/TUFFC.2011.1848.

[23] A. Reyes-Montero, L. Pardo, A. García, A. M. González, and M. E. Villafuerte-Castrejón, "$Ba_{1-x}Ca_xTi_{0.90}Zr_{0.10}O_3$ shear properties and their frequency dependence determined from ceramic plates by an effective method for resonance decoupling," *J. Alloys Compounds*, vol. 806, pp. 428–438, Oct. 2019, doi: 10.1016/j.jallcom.2019.07.210.

[24] S. Sherrit, T. J. Masys, H. D. Wiederick, and B. K. Mukherjee, "Determination of the reduced matrix of the piezoelectric, dielectric, and elastic material constants for a piezoelectric material with C_∞ symmetry," *IEEE Trans. Ultrason., Ferroelectr., Freq. Control*, vol. 58, no. 9, pp. 1714–1720, Sep. 2011, doi: 10.1109/TUFFC.2011.2008.

[25] N. Pérez, A. García, E. Riera, and L. Pardo, "Electromechanical anisotropy at the ferroelectric to Relaxor transition of $(Bi_{0.5}Na_{0.5})_{0.94}Ba_{0.06}TiO_3$ ceramics from the thermal evolution of resonance curves," *Appl. Sci.*, vol. 8, no. 1, p. 121, Jan. 2018, doi: 10.3390/app8010121.

[26] L. Pardo, A. García, K. Brebøl, E. Mercadelli, and C. Galassi, "Piezoelectric properties of lead-free submicron-structured $(Bi_{0.5}Na_{0.5})_{0.94}Ba_{0.06}TiO_3$ceramics from nanopowders," *Smart Mater. Struct.*, vol. 19, no. 11, Nov. 2010, Art. no. 115007, doi: 10.1088/0964-1726/19/11/115007.

[27] *EMAS-6100: Electronic Test Methods for the Characterisation of Piezoelectric Ceramic Oscillators*, Standard Electron. Mater. Manufacturers Assoc. Japan, Tokyo, Japan, 1993.

[28] K. Hikita, Y. Hiruma, H. Nagata, and T. Takenaka, "Shear-mode piezoelectric properties of $KNbO_3$-based ferroelectric ceramics," *Jpn. J. Appl. Phys.*, vol. 48, Jul. 2009, Art. no. 07GA05, doi: 10.1143/JJAP.48.07GA05.

[29] R. D. Mindlin, *An Introduction to the Mathematical Theory of Vibrations of Elastic Plates*, J. Yang, Ed. London, U.K.: World Scientific, 2006.

Pilar Ochoa-Pérez received the B.Sc. degree in physical sciences from the Complutense University of Madrid, Madrid, Spain, the M.Sc. degree in materials engineering from the Polytechnical University of Madrid (UPM), Madrid, in 1997 and 2000, respectively, and the Ph.D. degree from the School of Telecommunication Systems and Engineering, UPM, in 2006.

She is currently a Lecturer with the Department of Physical Electronics, Electrical Engineering and Applied Physics, School of Telecommunications Systems and Engineering, UPM. Her research activities included piezoelectric materials and their study by the finite-elements method.

Amador Miguel González-Crespo received the B.Sc. and Ph.D. degrees in physics from the Universidad Autónoma de Madrid (UAM), Madrid, Spain, in 1987 and 2004, respectively.

He carried out his bachelor's and doctoral theses with the Group of Ferroelectric Materials, Materials Science Institute of Madrid (ICMM-CSIC), Madrid. He is currently the Leader of the Section of Non-linear Dielectric Materials, POEMMA Research Group, "Universidad Politécnica de Madrid" (UPM), Madrid. He teaches undergraduate and graduate courses at the School of Telecommunication Systems and Engineering, where he is currently a Tenured Professor and the Dean. He is a member of the Senate and the Governing Council, UPM. He is interested in the development of new piezoelectric materials and devices based on piezoelectricity and ferroelectricity in the frame of sustainable development goals (more specifically 7, 9, and 13), to which he aims to contribute from his present position.

Dr. González is an Advisory Board Member of the Piezo Institute.

Álvaro García-Lucas was born in Madrid, Spain, in 1976. He received the B.Sc. degree in chemistry from the University of Madrid, Madrid, in 1998, and the Technician degree in telecommunication and informatics, IES, Madrid, in 2002.

He joined the present Materials Science Institute of Madrid, Spanish CSIC (ICMM-CSIC), Madrid, in 2004, where he has participated in research projects and networks of the European Commission (EC). He is currently a Computer Specialist with ICMM. He is also expert in the field of programming, particularly in coding and in the development of software for data acquisition and analysis in the characterization of polycrystalline ferroelectric materials.

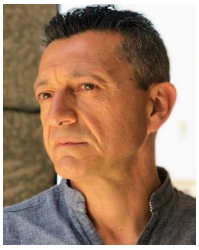

Francisco Javier Jiménez-Martínez received the Bachelor of Engineering degree from the Polytechnic University of Madrid, Madrid, Spain, in 1996, and the Ph.D. degree in telecommunication from the Polytechnic University of Madrid, Madrid, in 2003.

From 1988 to 1996, he was with the Spanish High Council of Scientific Research's (CSIC), Madrid. From 1996 to 1998, he was with Kodak, Madrid, where he was involved in medical imaging. He started his work in research and development at the POEMMA Research Group, Polytechnic University of Madrid, in 1996. Since 1998, he has been with the Polytechnic University of Madrid, where he is currently an Associate Professor with the School of Telecommunications Systems and Engineering, Department of Physical Electronics, Electrical Engineering and Applied Physics. He has been working in various projects, with private companies and government research centers, about ferroelectrics applications, automatic characterization systems, and virtual instrumentation.

Manuel Vázquez-Rodríguez received the Ph.D. degree in telecommunication from the Universidad Politécnica de Madrid (UPM), Madrid, Spain, in 2019.

He is currently an Associate Professor with the School of Engineering and Telecommunications Systems, Universidad Politécnica de Madrid (UPM), where he is also a Researcher with the CEMDATIC-POEMMA R&D Group. His current research interests include the functional applications of piezoelectric materials, power electronics, and energy harvesting systems.

Lorena Pardo was born in Madrid, Spain. She received the B.Sc. and Ph.D. degrees in physics from the "Universidad Complutense de Madrid," Madrid, in 1982 and 1987, respectively.

From 1984 to 1985, she was a Visiting Student with Materials Research Laboratory, Pennsylvania State University, State College, PA, USA. After this, she joined the Department of Ferroelectric Materials and become a Staff Member of the Spanish CSIC, Madrid, in 1989. She is Research Professor with the Materials Science Institute of Madrid (ICMM-CSIC). She was the Spanish Leader in several projects and Networks of the European Commission (EC) in collaboration with European industries. She has authored or coauthored some 220 publications on the topic. She works in the field of polycrystalline ferroelectric materials, processing, and multifunctionality.

Dr. Pardo was a member either of the Organizer or the Scientific Committees of the Spanish "Reunión Nacional de Electrocerámica" from the First Edition in 1991 and Co-Chaired the Third Edition in 1997 and Fourth Edition in 1999. She was a Co-founder of the "Electrocerámica" Section, Spanish Society of Ceramics and Glass, in 1998. She contributed to establish the European Institute of Piezoelectric Materials and Devices (Piezo Institute) in 2008 and is the Chair of its Advisory Board.